

Solidification Structure of Metastable Immiscible Cu–Fe Alloy Under Different Cooling Rates



Shichao Liu, Hang Li, Jinchuan Jie, Guomao Yin and TingJu Li

Abstract The experimental Cu–10 wt% Fe alloy was prepared by high frequency induction melting and arc melting, respectively. The corresponding microstructure and phase structure of alloy were investigated. The results show that the microstructure of the alloy prepared by high frequency induction melting exhibited Fe-rich droplets and Fe-rich dendrites developed in the copper matrix, suggesting the occurrence of the normal liquid-solid transformation as well as the liquid-liquid phase separation during solidification. Meanwhile the Oswald ripening and coagulation of Fe-rich droplets were also observed in the sample. Moreover, the Fe-rich droplets mainly segregated at the center of sample due to the combined effect of Stokes motion and Marangoni migration. However, the solidification microstructure of the alloy obtained by arc melting presented cellular Fe-rich dendrites in the copper matrix. There was no evidence of the liquid-liquid phase separation. Instead, the alloy experienced liquid-solid transformation during solidification. In general, all the experimental alloy are found to display a crystalline structure of BCC ϵ -Cu and FCC α -Fe.

Keywords Cu–Fe alloy · Solidification · Phase separation · Coagulation

Introduction

Cu–Fe alloys possess high strength and high thermal conductivity, as well as relative high electrical-conductivity, and also exhibits giant magnetoresistance and other outstanding physical properties [1–4]. Moreover, Fe is a common and cheap metal, widely used in daily life and industry, and also is abundant on Earth.

S. Liu · H. Li · J. Jie (✉) · G. Yin · T. Li
School of Materials Science and Engineering, Dalian University of Technology,
Dalian 116024, China
e-mail: jiejc@dlut.edu.cn

S. Liu
e-mail: liushichao0719@163.com

Therefore it has great potentials to be used as materials for magnetic recording, optical devices and sensors. Increasing interests have been paid to the Cu–Fe alloys in recent years. However, due to the existence of the metastable immiscible gap in the liquid state, Cu–Fe alloy is prone to take place the liquid-liquid separation, even under microgravity or zero gravity condition. Thus the preparation of the Cu–Fe alloy especially with high Fe content is still a challenge during the conventional solidification process, which certainly limits the application of the alloy. Therefore, more and more attention has been paid to the solidification behavior of the Cu–Fe alloy. Y. Nakagawa [5] studied the solidification behavior of Cu–Fe alloy under the undercooled condition, where he firstly found the liquid-liquid phase separation phenomenon. Since then, researchers calculated the thermodynamic properties and found that the Cu–Fe alloy shows a large and positive enthalpy of mixing [6, 7]. Chuang and Chen et al. [8, 9] calculated binary Cu–Fe phase diagram from the view of thermodynamics and confirmed the existence liquid immiscibility gap of alloy. He and Zhao et al. [10–12] manufactured different size of Powders of Cu–Fe alloy by using the high-pressure gas atomization technique to study microstructure evolution in the atomized droplets during solidification and also presented a model to quantitatively analyze the microstructural evolution during the metastable liquid–liquid phase separation. Wang and Shi et al. [13–15] prepared self-organized the core-shell or core-shell-core egg-typed microstructure by high-pressure gas atomization, meanwhile the corresponding formation mechanism of the microstructure was clarified and analyzed. Wang et al. [16] studied phase separation process of Cu–Fe melt from the view of molecular dynamics, and found the existence of inhomogeneity and segregation on atomic scale. In this present paper, the Cu–10 wt% Fe alloy is prepared by different methods. The obtained microstructure of the alloy was analyzed to study the solidification structure of metastable immiscible Cu–Fe alloy under different cooling conditions. Meanwhile the corresponding formation mechanism is also clarified in this article.

Experimental

The experimental Cu–Fe alloys were prepared by melting electrolytic copper (99.9% purity) and iron (99.97% purity). The alloy prepared by high frequency induction melting was carried out under the protection of argon gas, then the alloy was casted into a graphite mould with 20 mm in diameter and 50 mm in height. The alloy prepared by arc melting was also melt under the protection of argon gas. The alloys were repeatedly melted about several times to ensure sufficient mixing of all components for homogeneity. Then the alloy was directly solidified in a water-cooled copper hearth. In case of the different density of the Cu and Fe resulting in the buoyancy-driven floatation in experimental alloy, the specimens were sectioned in half, following the direction of gravity to get a representative view of the microstructures. The samples were then polished and etched by a solution consisting of 95 ml CH_2COOH , 5 ml HCl , and 5 g FeCl_3 . Microstructures

were observed by using an OLYMPUS GX51 optical microscope and a scanning electron microscope (SEM, Zeiss supra 55), equipped with an Energy Dispersive Spectrometer (EDS) operated at secondary electron mode and with an accelerating voltage of 15 kV. The chemical compositions of Fe-riches phases and the copper matrix were analyzed by SEM energy dispersive spectrometry (EDS), and the crystal structure of as-cast samples was characterized by an X-ray diffractometer (XRD, EMPYREAN with Cu radiation target) with the 2θ scan ranging from 20 to 100° at a speed of $4^\circ/\text{min}$.

Results and Discussion

Figure 1 shows the complete binary Cu–Fe alloy phase diagram including metastable miscibility gap [8, 9]. Cu–Fe is a typical kind of peritectic system, possessing a relatively flat liquidus and positive deviation from Raoul’s law. Thus the binary Cu–Fe alloy system exhibits a metastable immiscible gap which has already been proven both from thermodynamic calculation and experiment, as shown by dotted line in Fig. 1. If the alloy undercools into the metastable immiscible gap, the liquid–liquid phase separation would take place and would inevitably decompose into two liquids. Generally, the two liquids are immiscible with each other. As for a given composition alloy, whether metastable liquid–liquid phase separation occurs or not mainly depends on the degree of undercooling. In this paper, the interval between liquidus and the metastable liquid gap is defined as ΔT_{cu} . If the undercooling of the liquid alloy is less than ΔT_{cu} , the solidification of the alloy occurs above the miscibility gap boundary, and then the liquid–solid transformation occurs. The γ -Fe first solidifies as primary phase. Subsequently, the further cooling leads to the peritectic transformation at 1361 K, i.e. $\gamma\text{-Fe} + \text{L} \rightarrow \varepsilon\text{-Cu}$ and then the transformation of $\gamma\text{-Fe} \rightarrow \alpha\text{-Fe} + \varepsilon\text{-Cu}$ takes place at $T_{\alpha \leftrightarrow \gamma} = 1123$ K. If the undercooling of the liquid alloy exceeds ΔT_{cu} , the solidification occurs below

Fig. 1 The binary Cu–Fe alloy phase diagram

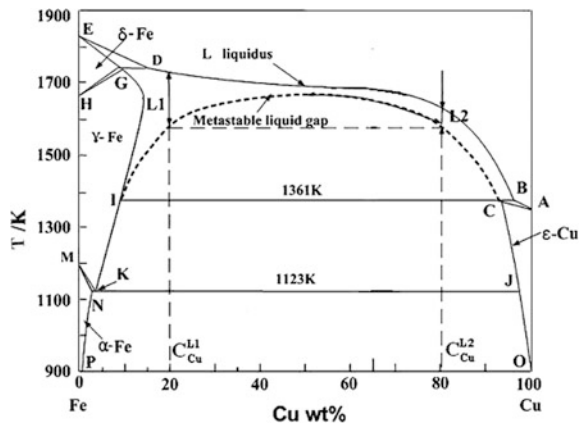
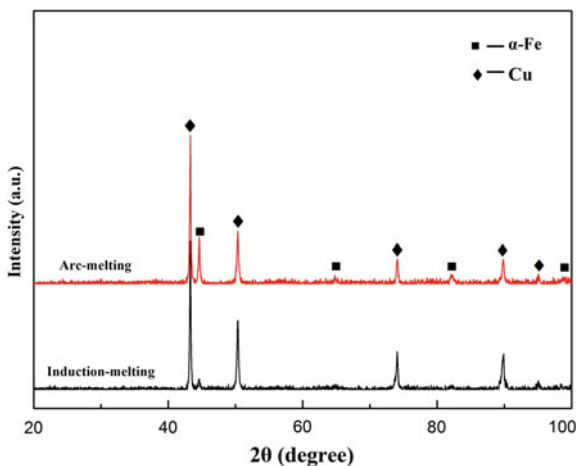


Fig. 2 XRD patterns of experimental prepared Cu–10 wt% Fe alloys



the miscibility gap boundary, the liquid–liquid transformation, so-called metastable phase separation, takes place. i.e. $L \rightarrow L_1(\text{Fe-rich}) + L_2(\text{Cu-rich})$. After liquid–liquid separation, the Fe-rich L_1 phase and the Cu-rich L_2 phase would follow different solidification paths due to the fact that each liquid experiences its own undercooling. Meanwhile, the Fe-rich phase L_1 phase would firstly solidify due to the large undercooling during the solidification.

Figure 2 presents XRD patterns of experimental prepared Cu–10 wt% Fe alloys by high frequency melting. All alloys display a crystalline structure of BCC ϵ -Cu and FCC α -Fe regardless of preparation method, which indicates that Cu has not reacted with Fe to form any intermetallic compounds.

Figure 3 shows the microstructure of the Cu–10 wt% Fe alloy obtained by high frequency melting. It can be clearly seen that the Fe-rich dendrites (Fig. 3b) uniformly and arbitrary distributed in the copper matrix. The random distribution of Fe-rich dendrites is mainly due to the uncertainty of the concentration fluctuation in alloy melt. In addition, a certain crystallographic relationship also exists between the primary dendrite arms in one nucleated dendrites. However, the dendrites formed by different nucleation doesn't exist a specific crystallographic orientation. Meanwhile, it can be also found that the spherical Fe-rich droplets (as magnified in Fig. 3c) exists in the Cu–10 wt% Fe alloy, with size ranging from 40 to 200 μm . As confirmed by the EDS analysis (shown in Fig. 3d), the Cu concentration in the spherical Fe-rich droplets is about 29.08 wt%, which results from of the liquid–liquid transformation.

According to the above analysis, if the actual undercooling of the alloy melt is not high enough to enter into the metastable immiscible gap, the alloy would solidify in normal liquid–solid transformation way. Thus the Fe-rich dendrites would precipitate. Therefore, most of the Cu–10 wt% Fe alloy melt solidified in graphite crucible has experienced the liquid–solid transformation and further solidified in the form the Fe-rich dendrites. However, if the actual undercooling of

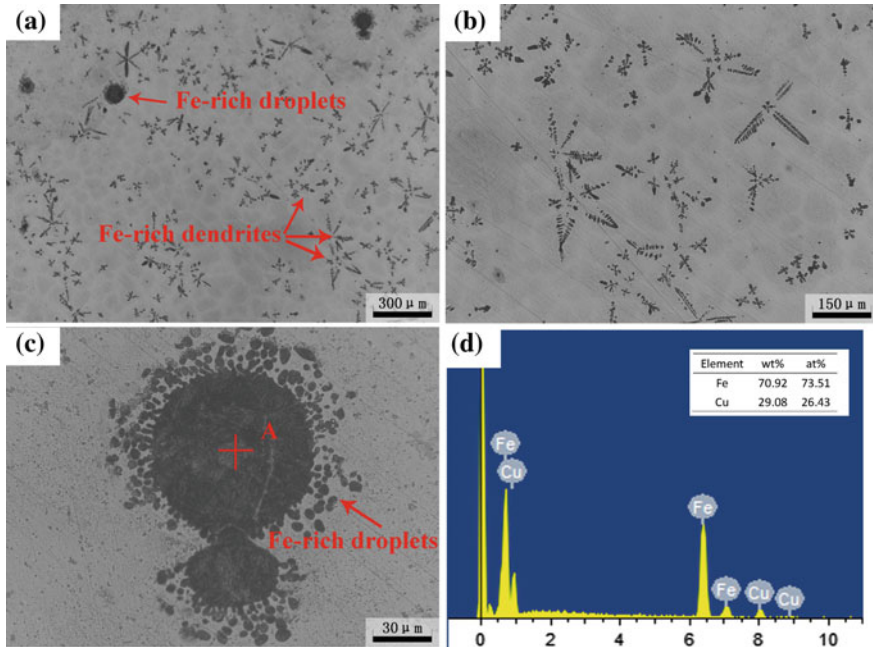


Fig. 3 Microstructure of Cu-10 wt% Fe alloy by high frequency induction melting, **b** and **c** are the enlarged image of **a**, **d** the EDS result of point A

the alloy melt can enter into the metastable immiscible gap, the liquid-liquid phase separation occurs, the alloy melt would separate into the Fe-rich and Cu-rich phase. The Fe-rich phase tends to form the spherical droplets in order to reduce the interfacial energy. Thus, the spherical Fe-rich droplets are the result of the liquid-liquid phase separation. In general, the Cu-10 wt% Fe alloy prepared by high frequency melting not only occurs the liquid-solid transformation but also undergoes the liquid-liquid phase separation.

Particular notable, an interesting phenomenon can be observed in Fig. 3c, the spherical Fe-rich droplets after the liquid-liquid phase separation are collided and coagulated with each other. Besides, many small spherical Fe-rich droplets surrounds and moves towards the nearest larger Fe-rich droplet, further suggesting the coagulation of the small Fe-rich droplets with the larger one after the liquid-liquid phase separation. According to the previous studies [10–15], the motion of the minor phase droplets is mainly controlled by Brown motion, Oswald ripening, Stokes movement and Marangoni migration. After the liquid-liquid phase separation, the minor phase droplets nucleated and formed the spherical droplets. At the beginning, due to the small radius of the minor phase droplets, the motion mainly depends on the Brown motion, and then undergoes Oswald ripening. However, when the radius of droplet increases to a certain extent, the Brown motion and Oswald ripening effect is not obvious. Instead, the motion of the droplets are

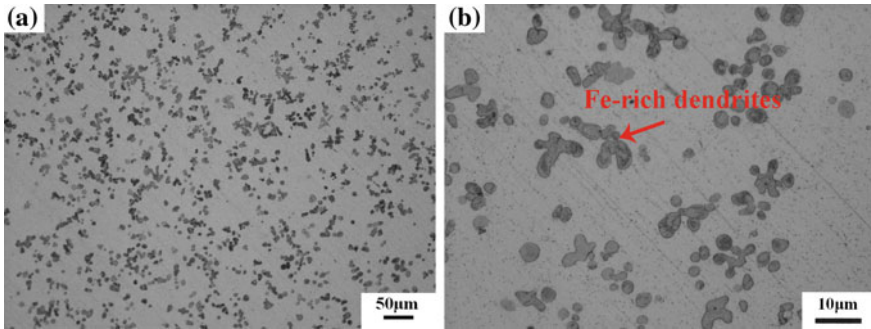


Fig. 4 Microstructure of Cu–10 wt%Fe alloy by arc-melting

dominated by the concurrent actions of the Marangoni migration and the Stokes motion. Meanwhile, both the velocity of Marangoni migration and the Stokes motion are proportional to the radius of Fe-rich droplets. Therefore, a large droplet may overtake a small one, thus the collision and coagulation would take place. As a result, during the moving process, each droplet is in collision with another and becomes larger in size. Consequently a new larger droplet would generate.

Figure 4 shows the microstructure of Cu–10 wt% Fe alloy prepared by arc melting. As can be seen, the Fe-rich dendrites uniformly and randomly distributed in the copper matrix, with size about 2–4 μm . Compared with the alloy prepared by high frequency melting, no developed dendrites can be found. Meanwhile there is no sign of spherical Fe-rich droplets, suggesting no occurrence of liquid-liquid phase separation in sample obtained by arc melting. Due to the high cooling rate, the Fe-rich dendrites show cellular morphology.

Summary

1. The Cu–10 wt% Fe prepared by high frequency melting not only undergoes the liquid-liquid phase but also undergoes the liquid-solid transformation. However, the liquid-liquid phase separation can't be found in the sample by arc melting. Moreover, both the experimental alloy display a crystalline structure of BCC $\varepsilon\text{-Cu}$ and FCC $\alpha\text{-Fe}$, regardless of preparation method.
2. The Cu–10 wt% Fe alloy obtained by high frequency melting shows well-developed Fe-rich dendrites after solidification. While the Cu–10%Fe alloy obtained by arc melting experienced the normal solidification phase and exhibits the finely cellular Fe-rich phases.
3. The liquid-liquid phase separation take place in the Cu–10 wt% Fe alloy prepared by high frequency melting. Meanwhile the Oswald ripening and coagulation process has been found due to Stokes motion and Marangoni migration.

Acknowledgements The authors gratefully acknowledge the supports of National Natural Science Foundation of China (Nos. 51501028, 51690163, 51471042, 51525401).

References

1. J.D. Verhoeven, S.C. Chueh, E.D. Gibson, Strength and conductivity of in situ Cu–Fe alloys. *J. Mater. Sci.* **24**(5), 1748–1752 (1989)
2. C. Biselli, D.G. Morris, Microstructure and strength of Cu–Fe in Situ, composites after very high drawing strains. *Acta Mater.* **44**(2), 493–504 (1996)
3. K. Liu, Z. Huang, X. Zhang et al., Influence of Ag micro-alloying on the thermal stability and ageing characteristics of a Cu–14Fe in-situ composite. *Mater. Sci. Eng. A* **673**, 1–7 (2016)
4. H. Gao, J. Wang, D. Shu et al., Effect of Ag on the microstructure and properties of Cu–Fe in situ composites. *Scr. Mater.* **53**(10), 1105–1109 (2005)
5. Y. Nakagawa, Liquid immiscibility in copper–iron and copper–cobalt systems in the supercooled state. *Acta Metall.* **6**(11), 704–711 (1958)
6. M.A. Turchanin, P.G. Agraval, I.V. Nikolaenko, Thermodynamics of alloys and phase equilibria in the copper–iron system. *J. Phase Equilib.* **24**, 307–319 (2003)
7. I.V. Nikolaenko, M.A. Turchanin, Enthalpies of formation of liquid binary (copper + iron, cobalt, and nickel) alloy. *Metall. Mater. Trans. B* **28**(6), 1119–1130 (1997)
8. Y.Y. Chuang, R. Schmid, Y.A. Chang, Thermodynamic analysis of the iron–copper system I: the stable and metastable phase Equilibria. *Metall. Trans.* **15A**(10), 1921–1930 (1984)
9. Q. Chen, Z. Jin, The Fe–Cu system: a thermodynamic evaluation. *Metall. Mater. Trans. A* **26**(2), 417–426 (1995)
10. J. He, J. Zhao, Behavior of Fe-rich phase during rapid solidification of Cu–Fe hypoperitectic alloy. *Mater. Sci. Eng. A* **404**, 85–90 (2005)
11. J. He, J.Z. Zhao, X.F. Wang et al., Microstructure development in finely atomized droplets of copper–iron alloys. *Metall. Mater. Trans. A* **36**(9), 2449–2454 (2005)
12. J. He, J.Z. Zhao, Solidification microstructure and dynamics of metastable phase transformation in undercooled liquid Cu–Fe alloys. *Acta Mater.* **54**, 1749–1757 (2006)
13. P.W. Cui, J.L. Xing, P.S. Rong et al., Design and formation mechanism of self-organized core/shell structure composite powder in immiscible liquid system. *Appl. Phys. Lett.* **91**(14), 141904–141904-3 (2007)
14. R.P. Shi, Y. Wang, C.P. Wang et al., Self-organization of core-shell and core-shell-corona structures in small liquid droplets. *Appl. Phys. Lett.* **98**(20), 204106–204106-3 (2011)
15. C.P. Wang, X.J. Liu, I. Ohnuma et al., Formation of immiscible alloy powders with egg-type microstructure. *Sci.* **297**(5583), 990–993 (2002)
16. H.P. Wang, B.B. Wei, *Chin. Sci. Bull.* **56**, 3416 (2011)